

IONIC CONDUCTIVITY OF Ag_2SO_4 DOPED WITH TRANSITION METAL AND RARE EARTH ION IMPURITIES

K SINGH, S M PANDE⁺, S W ANWANE⁺⁺ AND S S BHOGA^{*}

Department of Physics, Amravati University, Amravati 444 602, INDIA

+ Department of Physics, R.K.N. Engineering College, Nagpur - 440 013, INDIA

++ Department of Physics, Nagpur University, Nagpur - 440 010, INDIA

* Department of Physics, Hislop College, Nagpur - 440 001, INDIA

The ionic conductivity of $(1-x)\text{Ag}_2\text{SO}_4:(x)\text{MSO}_4$ and $(1-x)\text{Ag}_2\text{SO}_4:(x)\text{Me}_2(\text{SO}_4)_3$ (where $x=0$ to 0.1 , $M=\text{Co}$, Ni , Mn , Cu and $\text{Me}=\text{La}$, Y , Dy , Sm , Gd) has been systematically investigated by using complex impedance spectroscopy. The solid solubility limits of impurity cation in $\beta\text{-Ag}_2\text{SO}_4$ have been set with XRD and SEM. The ion transport number obtained by Wagners dc polarization method shows invariance over doping. The partial replacement of Ag^+ by wrong size cations causes lattice distortion which has been used to understand variation in activation enthalpy of ion migration.

Keywords: Solid electrolyte, solid solution, defect, activation enthalpy and silver sulphate

INTRODUCTION

Amongst sulphate based solid electrolytes, silver sulphate is less studied. It undergoes a phase transition from high temperature highly conducting hexagonal phase to low temperature moderately conducting orthorhombic β -phase at 689 K. In the recent past, ever since the concept of using metal/metal sulphate reference electrode in solid electrochemical gas sensors was evolved, it has evoked a remarkable attraction. It exhibits many fold advantages over other sulphate based solid electrolytes in engineering SO_2 gas sensors like; (i) coexistence of Ag-O-S phase in $\text{Ag}/\text{Ag}_2\text{SO}_4$ (ii) equilibration of antagonist SO_4^{2-} (solid) with SO_2/SO_3 (gas), (iii) high ionic conductivity invariant over SO_x environment etc. [1-4].

According to Höfer et al, aliovalent cation doping gives enhancement in conductivity in high temperature phase of Na_2SO_4 irrespective of its ionic size [5]. In contrast, while our earlier investigations reveals that in addition to valence, the ionic size and electronic structure of doped cations do play an important role in ion transport through the solid in low temperature phases of sulphates [6-9].

The present work attempts a systematic study on influence of lattice distortion and role of electronic structure caused

by d- block and rare-earth cations on Ag^+ mobility in $\beta\text{-Ag}_2\text{SO}_4$ to understand the fundamental conduction mechanism and simultaneously optimize an apt single phase silver sulphate based material for SO_2 gas sensor. The host lattice, Ag_2SO_4 , is expected to undergo the distortion upon the partial substitution of a wrong size cation (having ionic radius different than the host cation) within the limits of solid solution. Such a lattice distortion caused by host ion replacement is localised and expected to open doorways to form interconnected percolation channels (at threshold concentration) in which the Ag^+ hops from one site to nearby vacant site, the site occupation energies being equal.

EXPERIMENTAL

The appropriate mole fractions of the initial ingredients Ag_2SO_4 , MSO_4 and $\text{Me}_2(\text{SO}_4)_3$ (where $M=\text{Co}$, Ni , Mn , Cu and $\text{Me}=\text{La}$, Y , Dy , Sm , Gd) were prepared by slow cooling technique as discussed elsewhere [10]. The partial replacement of Ag^+ by M^{2+} or by Me^{3+} is made with a view to distorting the host lattice while creating extrinsic vacancies on the basis of the following formulae:

- (i) $\text{Ag}_{2-2x}\text{M}_x\text{SO}_4$ for the former
- (ii) $\text{Ag}_{2-3x}\text{Me}_x\text{SO}_4$ in case of the latter.

TABLE I: A comparison of experimental d and I/I_0 values with JCPDS data for the systems $(1-x)\text{Ag}_2\text{SO}_4:(x)\text{MSO}_4$ and $(1-x)\text{Ag}_2\text{SO}_4:(x)\text{Me}_2(\text{SO}_4)_3$ resulting in 5 vacancy %, where $M = \text{Co, Cu, Mn, Ni}$ and $\text{Me} = \text{La}$

AcO5		ACu5		AMn5		ANi5		ALa5		JCPDS DATA		[hk]	PHASE
d	I/I_0	d	I/I_0	d	I/I_0	d	I/I_0	d	I/I_0	d	I/I_0		
4.704	8	4.706	10	4.722	9	—	—	4.718	8.3	4.699	10	111	AS
3.997	15	3.997	20	4.013	21	4.016	24	4.006	10.1	3.994	25	220	AS
3.175	100	3.177	100	3.174	100	3.179	100	3.1842	100	3.177	70	040	AS
2.879	56	2.877	48	2.881	75	2.895	77	2.8751	46.4	2.873	100	311	AS
2.647	40	2.645	37	2.653	64	2.641	19	2.6594	20	2.644	90	022	AS
2.533	12	2.535	6	2.538	18	2.542	26	—	—	2.53	17	400	AS
2.424	20	2.423	1	2.431	18	2.43	29	2.4257	18.4	2.421	20	331	AS
1.926	19	1.927	18	1.928	24	—	—	1.9251	14.3	1.926	30	351	AS
1.915	8	1.915	11	1.917	10	1.918	22	—	—	1.915	12	511	AS
1.712	12	1.713	11	1.714	16	1.719	18	—	—	1.712	17	062	AS
1.672	12	1.672	8	1.676	17	—	—	—	—	1.673	12	313	AS
1.567	9	1.568	9	—	—	—	—	—	—	1.567	13	333	AS
1.546	7	1.546	8	1.546	9	1.549	9	—	—	1.546	8	371	AS

AS = $\beta\text{-Ag}_2\text{SO}_4$ JCPDS files No. 27-1403 Orthorhombic Ag_2SO_4

The prepared samples were characterized by X-ray powder diffraction (XRD) (Philips PW 170 diffractometer attached with PW 1710 controlling unit) using $\text{CuK}\alpha$ radiation, scanning electron microscope (SEM) (Cambridge Mark-III stereoscan electron microscope).

For electrical characterization, the specimens were obtained in the form of circular discs of 9 mm dia and 2 mm thick by pressing the powder with the help of specac (UK) stainless steel die-punch and hydraulic press. Thus obtained pellets were sintered at 773 K for 24 hrs. A good ohmic contact was ensured by using a quality silver paint onto both opposite parallel surfaces of pellet followed by baking at 473 K for 2 hrs. The real and imaginary parts of impedance were measured as a parametric function of frequency in the range from 5 Hz to 13 MHz and temperature from 723 to 523 K during cooling cycle using hp 4192A Impedance analyzer.

The ionic transference number of the specimens was measured by Wagners dc polarization method in the temperature range from 673 to 573 K with the help of Keithley SMU 236 with the cell configuration;

Pt/Electrolyte/Ag

RESULTS AND DISCUSSION

A comparison of experimental interplaner distance, d , and relative intensity of characteristic line, I/I_0 , values for various di- and tri-valent doped Ag_2SO_4 with those of JCPDS (joint committee for powder diffraction society) data is given in Table I. As is evident, a general shift in d -values for doped systems in comparison with that for pure Ag_2SO_4 is worthwhile to note. This shift is, in general, attributed to incorporation of 'wrong' size cation in the host lattice which may also alter the relative intensity corresponding to 'd'

TABLE II: Lattice cell constants for $(1-x)\text{Ag}_2\text{SO}_4:(x)\text{MSO}_4$ and $(1-x)\text{Ag}_2\text{SO}_4:(x)\text{Me}_2(\text{SO}_4)_3$ system resulting in 5 vacancy % where $M = \text{Co, Cu, Mn, Ni}$ and $\text{Me} = \text{La}$

System at 5V%	a Å	b Å	c Å	Volume Å ³	Ionic radius Å
Ag_2SO_4	10.247	12.693	5.830	758.429	1.26
$+\text{La}_2(\text{SO}_4)_3$	10.255	12.704	5.811	757.054	1.15
$+\text{MnSO}_4$	10.258	12.694	5.809	756.419	0.80
$+\text{CoSO}_4$	10.252	12.684	5.804	754.731	0.74
$+\text{NiSO}_4$	10.251	12.688	5.817	756.586	0.72
$+\text{CuSO}_4$	10.249	12.683	5.800	753.930	0.69

values. The absence of any line corresponding to either MSO_4 or $\text{Me}_2(\text{SO}_4)_3$ (or any intermediate phase) for $x \leq 0.0527$ and $x \leq 0.0363$ respectively indicates solid solubility. The local distortions caused by the 'wrong' size substitutions are substantiated by the change in magnitude of unit cell constants as presented in Table II.

Microphotographs representing the surface morphology of pure and doped Ag_2SO_4 revealed that the grain morphology is more or less unaltered with impurity addition for $x \leq 0.0527$ and $x \leq 0.0363$ in case of di- and trivalents doped Ag_2SO_4 respectively. Also, precipitation of any impurity phase is not observed in this region. Further addition of M and Me (i.e. for vacancy concentration 7%) results in the precipitation of fine distinguishable impurity grains which increases in quantity with rise in its concentration. These results are in good agreement with XRD analysis.

In orthorhombic phase for almost all compositions a distorted semicircular arc is observed in the complex impedance plane. A nonlinear least squares fit method is used to obtain conductivity data i.e bulk conductivity, activation enthalpy and pre-exponential factor.

All compositions obey Arrhenius law within the range of temperature of interest

$$(\sigma T) = (\sigma T)_0 \exp \left(\frac{-E_a}{kT} \right) \quad (1)$$

where, $(\sigma T)_0$ is pre-exponential factor and other parameters have usual meaning.

Figs. 1(a) and 1(b) respectively show the concentration dependent conductivity for various d-Block elements (di-valents) and rare earth elements (tri-valents) doped

Ag_2SO_4 . The conductivity for both these series rises with vacancy concentration up to about 5% and decreases thereafter.

The conductivity behaviour in $(1-x) \text{Ag}_2\text{SO}_4 \cdot (x) \text{MSO}_4$ systems is anomalous, particularly in the light of the fact that M^{2+} has a much smaller ionic radius than that of Ag^+ . The results pertaining to this system could be explained qualitatively on the basis of electronic structure of dopant as follows:

It is worthwhile to note that these elements belong to the d-Block and are grouped in 3d class of elements which are transition metals. Accordingly, each of these cations belonging to d-Blocks distinctly has got its own particular electronic cloud and the corresponding distinct potential contours while it occupies a lattice site in Ag_2SO_4 matrix by way of solid solution. It was suggested that the quadrupolar polarizability of mobile metal ions may reduce the energy barrier associated with the motion along mobile ion pathways from the minima at the site of high symmetry to the energy barrier at the site of lower symmetry [11]. This implies that for 'isostructural' materials, mobile ions with high quadrupolar polarizability should be relatively more mobile compared to ions with lower quadrupolar polarizability [12]. The Ag^+ which is indeed a mobile ion may get more polarized due to probable deformation of charge cloud, when made to pass through the potential contours surrounding the "3-d-Block" dopant cation (M^{2+}). This will impart a higher mobility to the Ag^{2+} in spite of the lattice contraction (Table II) taking place on account of fractional r_g/r_h ratio. Owing to this 'distortion' the corresponding activation energy should be more than that of the host. Fig. 2 represents the dependence of activation energy on the ionic size of the guest cation which exhibits minimum for a threshold ionic

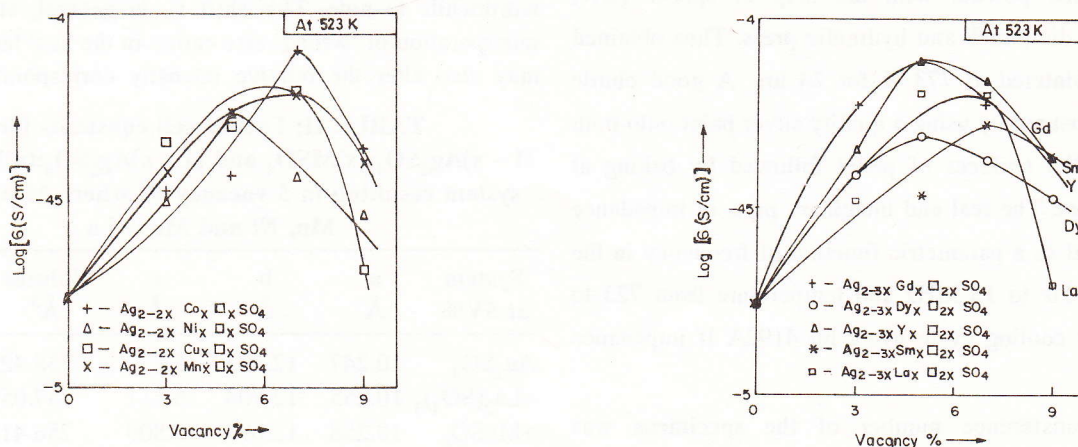


Fig. 1: Variation of $\log(\sigma)$ as a function of vacancy % concentration for (a) $\text{Ag}_{2-2x}\text{Me}_x\text{SO}_4$ and (b) $\text{Ag}_{2-3x}\text{M}_x\text{SO}_4$ systems at 523 K

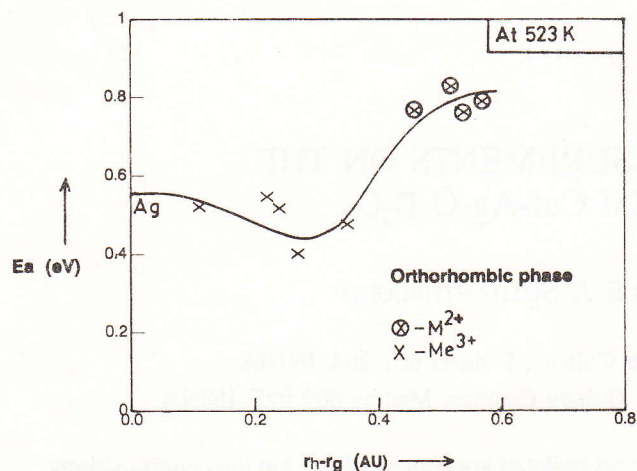


Fig. 2: Variation of activation energy, E_a with difference in ionic size ($r_h - r_g$) at 523 K for 5 vacancy % concentration of $(1-x)\text{Ag}_2\text{SO}_4:(x)\text{MSO}_4$ and $(1-x)\text{Ag}_2\text{SO}_4:(x)\text{Me}_2(\text{SO}_4)_3$ systems

size of the dopant which opens the silver ion percolating inter-connected channels resulting into optimum ionic conductivity. Interestingly, however, the mobile Ag^+ will contribute largely to the conductivity owing to number of extrinsic vacancies available and polarization because of substitution of a M^{2+} in Ag_2SO_4 matrix. Similar findings in $\beta\text{-Li}_2\text{SO}_4$ show that a larger activation energy is associated with the small sized dopants [13]. The dependence of ionic conductivity with dopant concentration in $(1-x)\text{Ag}_2\text{SO}_4:(x)\text{Me}_2(\text{SO}_4)_3$ system can be understood as follows:

Confirming to the formula (ii), there are two additional extrinsic cationic vacancies in the close vicinity of the impurity (Me^{3+}) which partially substitutes Ag^+ in the host lattice. Furthermore, since Me^{3+} has a lower ionic radius than Ag^+ , this substitution facilitates localized lattice contraction (Table II). Nevertheless, a large ionic conductivity in these samples is attributed to the availability of additional extrinsic vacancies to the mobile Ag^+ (Fig. 1(b)). Here, we have simplified the model by neglecting the impurity-vacancy association. With increasing vacancy concentrations due to partial substitutions of Me^{3+} , the probability of successive cationic jumps increases, which, in turn, increases the conductivity. Upon further addition, $x \geq 0.0363$ (i.e. beyond 7 vacancy % concentration) the mobility of Ag^+ is reduced following vacancy-vacancy interactions such as cluster formation and also cationic sublattice ordering [5]. These opposite effects cancel each other at conductivity maximum about 7 vacancy % and contribute in reducing Ag^+ mobility

in rest of the region (i.e. $0 < \text{vacancy \%} < 7$ and $7 < \text{vacancy \%} < 10$). However, within solid solubility limits, these two different probable physical processes viz. the availability of extrinsic vacancies and the localized distortion produce the net effect in such a sense that the activation energy of the doped samples is nearly unaffected which is clearly evident from Fig. 2.

CONCLUSION

Modifying the lattice by mere substitution is not only criterion to enhance the ionic conductivity, but selection of proper size is important. Secondly, the electronic configuration of the dopant ion should be taken in account, since it also plays a vital role. Moreover, if charge cloud of mobile ion is deformable (i.e. polarizabilities are relatively high) by impurity substitution, the energy barriers associated with charges in coordination environment, as particle moves along conduction path, will be smaller or greater depending on size. The optimized material may be considered for engineering of galvanic SO_2 gas sensors.

Acknowledgement: The authors are thankful to CSIR, New Delhi for providing financial assistance to carry out this work.

REFERENCES

1. Q G Liu and W L Worrell, *US Patent Applic*, 303-320 (Sep 17), (1981) p 17
2. W L Worrell and Q G Liu, *J Electronal Chem*, 168 (1984) 355
3. C M Mari, M Beghi and S Pizzini, *Sensors and Actuators B*, 2 (1990) 51
4. K Singh, S W Anwane, U K Lanje and S S Bhoga, *Proc 5th National Symposium on Environment*, Eds V N Sastry, V N Bapat and M V M Desai, Feb 29 (1996) 214
5. H H Hofer, W Eysel and U V Alpen, *J Solid State Chem*, 36 (1981) 365
6. K Singh and S S Bhoga, *Solid State Ionics*, 39 (1990) 205
7. K Singh, S S Bhoga and S W Anwane, *J Applied Physics*, (1996) (In press)
8. K Singh, S S Bhoga and S W Anwane, *Solid State Ionics*, (1996) (In press)
9. K Singh, *Solid State Ionics*, 28-30 (1988) 1371
10. K Singh, S M Pande and S S Bhoga, *J Solid State Chem*, 116 (1995) 232
11. W G Kleppmann and H Blitz, *Comm Phys*, 1 (1976) 105
12. M A Ratner, A Nitzan, *Solid State Ionics*, 28-30 (1988) 3
13. A Lunden and R Tärneberg, *Proc 4th Asian Conf on Solid State Ionic*, Eds B V R Choudhary, (1994) 3